

Tooth Contact Analysis of Involute Beveloid Gear Based on Higher-Order Curve Axial Modification

Yongping Liu[1,2] ✉ – Qi Chen[1] – Changbin Dong[1]

1 Lanzhou University of Technology, School of Mechanical and Electrical Engineering, China
2 Lanzhou University of Technology, State Wenzhou Engineering Institute of Pump & Valve, China
✉ cameliu@163.com

Abstract *This study investigates the tooth flank contact characteristics of a beveloid gear pair through the lens of higher-order curve tooth modification of the involute beveloid gear. The machining coordinate system of the modified gear pair is established, and its tooth surface equations are derived based on the principle of gear meshing and coordinate transformation. In this context, a contact analysis of the modified gear is conducted, examining the impact of varying parameters on the contact trace and contact ellipses, as well as the implications for meshing characteristics in the presence of assembly errors. The findings indicate that the contact form of the high-order curve axial modification of the beveloid gear pair is point contact. Furthermore, the maximum modification magnitude and the order of the modification curve influence the meshing performance of the beveloid gear pair. Additionally, the beveloid gear pair demonstrates enhanced tolerance to the center distance and the axis crossed error, while exhibiting reduced tolerance to the axis intersected error.*

Keywords *involute beveloid gear, higher order curve axial modification, tooth contact analysis, transmission error, assembly error*

Highlights

- *The model of involute beveloid gear pair with higher-order curve axial modification is constructed.*
- *The contact paths and contact ellipses of the modified beveloid gear pair are derived.*
- *The transmission error of the modified gear pair is calculated.*
- *The transmission error difference of the modified gear pair with different assembly errors is analyzed.*

1 INTRODUCTION

Involute beveloid gears offer a number of advantages, including ease of manufacture, low cost and high accuracy. As a result, they are suitable for a range of applications, including fast ferries, all-drive automobiles, aerospace precision machinery and other instances of power transmission. However, the beveloid gear pair exhibits transmission error, uneven contact stress distribution, and other factors during operation, which result in vibration impact and a reduction in load-bearing capacity and transmission performance. Consequently, there is a need to enhance the durability of the gear pair's surface and improve its load-bearing transmission performance.

The load-bearing capacity represents a crucial criterion for evaluating the performance of gear transmissions. The accuracy of the model of tooth contact stress and inter-tooth load distribution coefficient is a fundamental prerequisite for ensuring the precision of the calculated results of gear bearing contact mechanics [1]. Modification can effectively enhance the gear dynamic load change gradient, mitigate shock, vibration and noise, and thus improve the quality of gear transmission. Axial modification is one of the methods of tooth modification, which can also be termed micro-geometric design. It is an effective approach to augment such performance.

The modelling of involute beveloid gears provides the foundation for related research. Chen et al. [2] proposed a method for machining a straight-toothed beveloid internal gear pair with tooth blanks parallel to the gear shaping tool. Additionally, they derived theoretical models for the beveloid internal gear and the beveloid external gear, and conducted a load-bearing contact analysis. Sun et al. [3] put forth a novel approach to modelling the tooth surface of involute beveloid gears, employing the theory of minimum potential energy in conjunction with the slicing method. They also investigated the impact of design parameters on the contact characteristics of parallel axis beveloid gears. Şentürk and Fetvacyi [4] developed a mathematical method for the prevention of root cuts on the model of beveloid gears. They also developed a mathematical method for the prevention of root cuts on the model of parallel shaft variable thickness gears. Furthermore, they developed a mathematical method for the prevention of root cuts generated on beveloid gear.

The meshing stiffness is also a frequently studied topic in the digital modelling of gears. Wen et al. [5] derived the contact line equations of a parallelled beveloid gear pair, proposed an analytical algorithm for calculating the meshing stiffness of a beveloid gear based on the slicing method, and analyzed the effect of changing parameters on the meshing stiffness of a beveloid gear. Song et al. [6] put forth a methodology for calculating the meshing stiffness of parallelled beveloid gears based on the potential method. They also investigated the impact of parameters such as pressure angle, pitch cone angle, gear displacement coefficient, and others. Zhou et al. [7] developed an alternative meshing stiffness model that considered the influence of parameters like the direction of inter-tooth friction. The influence of specific parameters on the meshing stiffness was examined, including pressure angle, pitch cone angle, and gear displacement coefficient. Mao et al. [8] enhanced the existing Weber energy method, which is based on the gear slicing method, constructed a time-varying mesh stiffness solution model for involute beveloid gears, and calculated and verified the time-varying meshing stiffness of beveloid gears. Liu et al. [9] constructed a three-dimensional model of a beveloid gear transmission and a gear dynamics model of a parallelled beveloid gear, based on the processing principle of a beveloid gear. They then proceeded to analyse the influence factors of the transmission error of a beveloid gear.

The microgeometric design of the beveloid gear, also referred to as the modification of the beveloid gear tooth, has constituted

 DOI: 10.5545/sv-jme.2024.1254

a significant field of investigation in recent years. Wang et al. [10] put forth a methodology for calculating modifications to tooth profiles for the purpose of analysing tooth contact. Fuentes et al. [11] proposed an enhanced solution for intersecting beveloid gears with two distinct types of tooth profile bulge modification, with the objective of enhancing load-carrying capacity and reducing noise and vibration response. Şentürk et al. [12] developed a computer programme to obtain generating and generated surfaces of beveloid gears with modification. Morikawa et al. [13] examined the impact of tooth profile modifications on tooth surface damage through the utilization of a tooth fatigue test. In a further contribution to the field, Brecher et al. [14] put forward a method for the design of the tooth surface of intersected beveloid gears, taking into account the tolerance field for functional tolerance. Brimmers et al. [15] also made a significant contribution to the design of tooth flanks of variable thickness gears, investigating the possibility of free flank modification by means of a weighted objective function of beveloid gears with respect to the operating behavior. Ni et al. [16] designed a rack cutter with a parabolic modification to enhance the contact characteristics of helical beveloid gears. They then proceeded to investigate the impact of the parabolic modification on the contact path and contact ratio. Finally, they conducted an in-depth analysis to determine the sensitivity of beveloid gears to mounting errors. Liu et al. [17] put forth a numerical design methodology to augment the meshing characteristics of alternated beveloid gears through modification on the contact ellipse, contact path, transmission error, and relative curvature. Cao et al. [18] introduced the rack cutter with parabolic modification into the design of intersected beveloid gear pairs and investigated the effects of the modification coefficients on the mesh characteristics of the gear pair, including contact mode, transmission error, mesh stiffness, contact force, and tooth root stress. Zhang et al. [19] proposed a differentiated modification method based on a sine function, analyzed the dynamic characteristics and noise of gear pairs, comparing unmodified, normally, and differentially modified gears.

Presently, the majority of modification designs for involute beveloid gears are based on previous design experience. Consequently, the innovative modification method for beveloid gears is of great significance, as it offers a promising avenue for enhancing the meshing characteristics of beveloid gear pair. The involute parallelled beveloid gear is distinguished by a distinctive tooth surface configuration, which exhibits the phenomenon of automatic backlash adjustment. However, modifications to this configuration are not recommended for significant alterations in the central portion of the tooth surface. Instead, high-order curves are employed to the axial modification, resulting in a notable discrepancy between the two ends and a relatively minor discrepancy in the central region. This paper derives the mathematical equations of the tooth surface of the beveloid gear under the corresponding design parameters, including the maximum amount of thickened gears. It clearly outlines the design steps of the modelling method of the high-order curve axial modification model and carries out a tooth contact analysis (TCA) for the modification of the parallelled beveloid gear. This aims to establishing a perfect modification theory of the involute parallelled beveloid gear transmission and promoting the development and application of the beveloid gear.

2 METHODS & MATERIALS

The tooth profiles of the involute beveloid gear, as they exist in their unmodified state, can be considered to be generated under the tooth profile envelope of a usual rack cutter. In accordance with this principle, the tooth surface equations of the beveloid gear can be derived by undertaking a series of coordinate transformations through the rack cutter surface equations, as illustrated in Fig. 1. In the figure, the angle formed by the normal coordinate system $S_n(x_n,y_n,z_n)$ and the end coordinate system $S_o(x_o,y_o,z_o)$ of the rack cutter is the helix angle β, while the angle formed by the end coordinate system S_o and the pitch coordinate system $S_c(x_c,y_c,z_c)$ is the pitch angle γ. Coordinate system $S_j(x_j,y_j,z_j)$ is a movable coordinate system attached to the blank of the beveloid gear, while coordinate system $S_b(x_b,y_b,z_b)$ is a stationary coordinate system with its origin located at the center of the end face of the blank of the beveloid gear. The coordinate origin position O_n of S_n is jointly determined by the variable $u=O_oO_n$ and the helix angle β. The angular velocity during the rotation of the beveloid gear blank is ω, the radius of the dividing cylinder of the beveloid gear is r, the translation speed of the rack cutter is $v=\omega\cdot r$, and the real-time rotation angle of the beveloid gear during the machining process is φ_j.

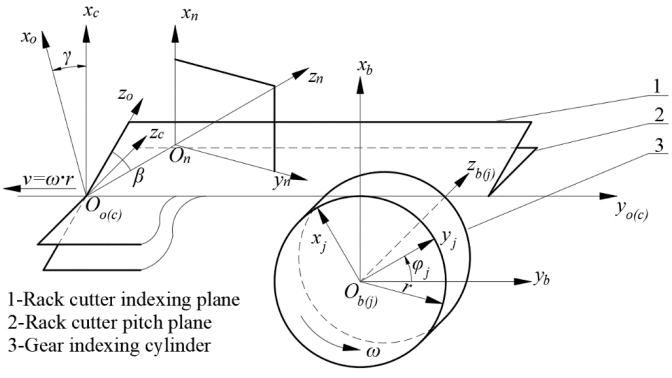

Fig. 1. Coordinate system for the generation of the beveloid gear

In the normal coordinate system S_n of the rack cutter, the normal tooth profile vector of the rack cutter is given by

$$\mathbf{r}_n=[x_n \quad y_n \quad z_n \quad 1]^{\mathrm{T}} \tag{1}$$

The rack cutter surface in the pitch coordinate system, designated S_c, can be obtained by combining the normal tooth profile vectors with the following coordinate transformations:

$$\mathbf{r}_c=\mathbf{M}_{cn}\mathbf{r}_n=[x_c \quad y_c \quad z_c \quad 1], \tag{2}$$

where $\mathbf{r}_c$ is the position vector of the rack cutter surface in the coordinate system S_n; The transformation matrix, designated as $\mathbf{M}_{cn}$, is employed for the purpose of effecting a change from the coordinate system S_n to the coordinate system S_c, and the transformation matrix is given by:

$$\mathbf{M}_{cn}=\begin{bmatrix} \cos\gamma & -\sin\beta\sin\gamma & \cos\beta\sin\gamma & u\cos\beta\sin\gamma \\ 0 & \cos\beta & \sin\beta & u\sin\beta \\ -\sin\gamma & -\cos\gamma & \cos\beta\cos\gamma & u\cos\beta\cos\gamma \\ 0 & 0 & 0 & 1 \end{bmatrix}. \tag{3}$$

The position vector $\mathbf{r}_c$ of the tooth face of the rack cutter in the section coordinate system S_c is combined with the relative motion relationship between the rack cutter and the gear blank during the machining process. Consequently, the equation representing the tooth face of the beveloid gear in coordinate system S_j is derived as:

$$\mathbf{r}_j:\begin{cases} x_j=x_c\cos\varphi_j-y_c\sin\varphi_j+r(\cos\varphi_j+\varphi_j\sin\varphi_j) \\ y_j=x_c\sin\varphi_j-y_c\cos\varphi_j+r(\sin\varphi_j+\varphi_j\cos\varphi_j) \\ z_j=z_c \\ \varphi_j=n_{xc}y_c-n_{yc}y_c/n_{xc}r \end{cases}, \tag{4}$$

where x_j, y_j, z_j represent the position vectors of the tooth surface of the beveloid gear, and n_{xc}, n_{yc} and n_{zc} denote the unit normal vectors of the rack cutter surface.

In accordance with the tooth equation, a computer program has been developed to generate the point set of the tooth profile of an involute beveloid gear. Figure 2 illustrates the point cloud model of the tooth profile of the beveloid gear with the parameters outlined in Table 1.

Table 1. Basic parameters of involute beveloid gears

Parameters	Pinion	Gear
Normal modules [mm]	2.5	
Center distance [mm]	80	
Pressure angle [°]	20	
Tooth number	27	37
Tooth width [mm]	26	24
Pitch angle [°])	6	6

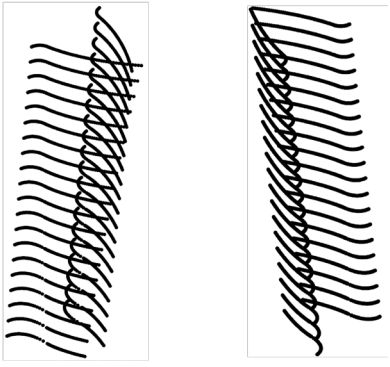

Fig. 2. Point cloud model of beveloid gear tooth surface

In the event of a high-order curve axial modification being applied on the involute beveloid gear, the amount of modification at each location in the axial direction can be expressed as follows:

$$\Delta_u = a_{m0}\left(\frac{1}{2}B - u\right)^2 + a_{m1}, \tag{5}$$

where a_{mi} represents the modification factor of gear thickness modification (i=0, 1), B denotes the length of the tooth width of the beveloid gear, and u signifies the distance from the end face in the axial direction at that specific point.

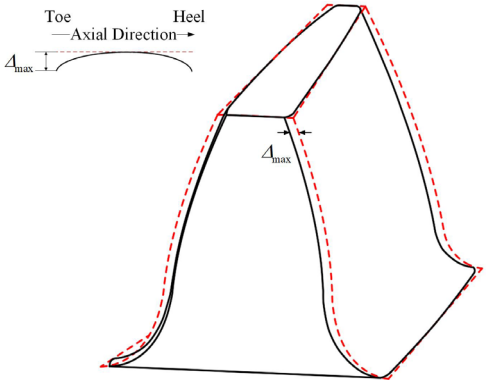

Fig. 3. Beveloid gear with higher order curve axial modification

Figure 3 illustrates the modification of the involute beveloid gear under conditions of high-order curve axial modification. The dotted and solid lines indicate the tooth surface of the beveloid gear before and after modification, respectively. The maximum modification magnitude of the beveloid gear is represented by Δ_{max}.

3 RESULTS AND DISCUSSION

3.1 Tooth Contact Analysis of Involute Beveloid Gear Based on High-Order Curve Axial Modification

Following the axial modification of the involute beveloid gear, the tooth face of the beveloid gear assumes a drum-shaped configuration, and the equations governing this tooth face exhibit greater complexity compared to those of the ordinary involute gear. In order to study the meshing characteristics, a meshing coordinate system is established for the beveloid gear. The TCA mathematical model of the involute beveloid gear pair is then obtained by transforming the coordinate system so that the modification of the pinion and the gear can achieve the correct meshing under this coordinate system.

In accordance with the tooth surface equation of the high-order curve axial modification of the beveloid gear outlined in the preceding section, the tooth position vectors $\mathbf{r}_p$ and $\mathbf{r}_g$ and normal vectors $\mathbf{n}_p$ and $\mathbf{n}_g$ of the pinion and gear can be derived using the following expressions:

$$\begin{cases} \mathbf{r}_p(u_p, v_p) = x_p\mathbf{i} + y_p\mathbf{j} + z_p\mathbf{k} \\ \mathbf{r}_g(u_g, v_g) = x_g\mathbf{i} + y_g\mathbf{j} + z_g\mathbf{k} \\ \mathbf{n}_p(u_p, v_p) = n_{px}\mathbf{i} + n_{py}\mathbf{j} + n_{pz}\mathbf{k} \\ \mathbf{n}_g(u_g, v_g) = n_{gx}\mathbf{i} + n_{gy}\mathbf{j} + n_{gz}\mathbf{k} \end{cases}, \tag{6}$$

where the functions x_p, y_p, z_p, n_{px}, n_{py}, and n_{pz} are defined with respect to two independent variables, u_p and v_p. Similarly, the functions x_g, y_g, z_g, n_{gx}, n_{gy}, and n_{gz} are defined with respect to two independent variables, u_g and v_g.

The beveloid gear pair transmission introduces two new variables, designated as ψ_p and ψ_g, which represent the position angles of the pinion and the follower, respectively. These variables satisfy the conditions at a ratio of i:

$$\psi_g / \psi_p = i. \tag{7}$$

Following the implementation of the high-order curve axial modification scheme, the configuration of tooth contact is characterized by point contact. Furthermore, the two position vectors and the two normal vectors of the two conjugate tooth surfaces at the contact point are equal [20]. In consequence, the mathematical model for contact analysis of a beveloid gear pair is given by:

$$\begin{cases} \boldsymbol{r}_p(u_p, v_p, \psi_p) = \boldsymbol{r}_g(u_g, v_g, \psi_g) \\ \boldsymbol{n}_p(u_p, v_p, \psi_p) = \boldsymbol{n}_g(u_g, v_g, \psi_g) \end{cases}. \tag{8}$$

The partial vectors in the x, y, and z directions corresponding to the position and normal vectors in Eq. (8) are equal. Furthermore, by coupling Eq. (7), four relatively independent sets of equations can be obtained. In the contact analysis calculation of the beveloid gear pair, the position angle ψ_p of the pinion can be regarded as a known quantity and solved separately by substituting a number of values within the meshing range. This results in the original set of equations becoming composed of four independent equations with four independent variables. Consequently, the solution to the set of contact equations can be achieved. The initial meshing point is designated as the reference point for calculation, and the resulting tooth contact trajectory points are shown as discrete red points in Fig. 4.

In order to analyze the contact area of the tooth surface of the beveloid gear pair, it is necessary to calculate the curvature of the tooth surface. The first-order and second-order partial derivatives of the position vector $\mathbf{r}$ can be derived from the first and second fundamental quantities of the surface, as follows:

$$\begin{cases} \mathbf{r}_u = \dfrac{\partial \mathbf{r}(u,v)}{\partial u} \\ \mathbf{r}_v = \dfrac{\partial \mathbf{r}(u,v)}{\partial u} \\ \mathbf{r}_{uu} = \dfrac{\partial^2 \mathbf{r}(u,v)}{\partial u^2} \\ \mathbf{r}_{uv} = \dfrac{\partial^2 \mathbf{r}(u,v)}{\partial u \partial v} \\ \mathbf{r}_{vv} = \dfrac{\partial^2 \mathbf{r}(u,v)}{\partial v^2} \end{cases}, \tag{9}$$

$$E = \mathbf{r}_u{}^2,\ F = \mathbf{r}_u \cdot \mathbf{r}_v,\ G = \mathbf{r}_v{}^2,$$
$$L = \mathbf{r}_{uu} \cdot \mathbf{n},\ M = \mathbf{r}_{uv} \cdot \mathbf{n},\ N = \mathbf{r}_{uu} \cdot \mathbf{n}, \tag{10}$$

$$\mathbf{n} = \frac{\mathbf{r}_t \times \mathbf{r}_v}{\left|\mathbf{r}_t \times \mathbf{r}_v\right|}, \tag{11}$$

where the $\mathbf{r}_u$ and $\mathbf{r}_v$ represent the first-order partial derivatives of the position vector $\mathbf{r}$ with respect to u and v, respectively. Meanwhile, $\mathbf{r}_{uu}$, $\mathbf{r}_{uv}$ and $\mathbf{r}_{vv}$ denote the second-order partial derivatives of the position vector $\mathbf{r}$. E, F, and G are the first fundamental quantities of the surface, and L, M, and N are the second fundamental quantities of the surface. The unit normal vector $\mathbf{n}$ at point (u, v) is given by Eq. 11.

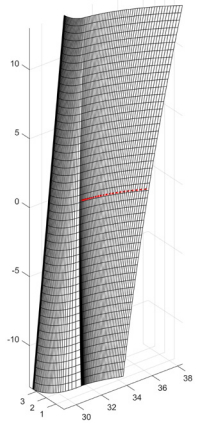

Fig. 4. Contact path for the tooth surface with high-order curve axial modification

The variation of curvature at the tooth contact point can be obtained from the principal curvature, which in turn allows for the calculation of the size and location of the contact area. The tooth profile direction principal curvature (K_1) and the tooth width direction principal curvature (K_2) are solved by the Gaussian curvature (K) and the mean curvature (H). This process is described by Eqs. (12) to (15):

$$K = \frac{LN - M^2}{EG - F^2}, \tag{12}$$

$$H = \frac{LG - 2MF + NE}{2(EG - F^2)}, \tag{13}$$

$$K_1 = H + \sqrt{H^2 - K}, \tag{14}$$

$$K_2 = H - \sqrt{H^2 - K}. \tag{15}$$

The tooth contact form of the beveloid gear with high-order curve axial modification is characterized by point contact. However, in actual conditions, this contact will extend into an elliptical contact area due to elastic deformation, as illustrated in Fig. 5.

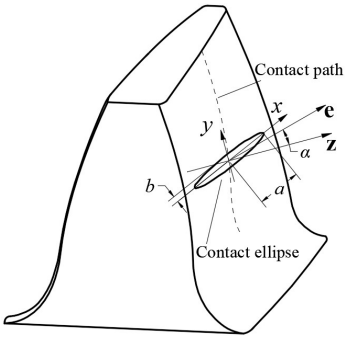

Fig. 5. Tooth contact area

In Figure 5, a and b represent the lengths of the semi major axis and semi minor axis of the contact ellipses, respectively. The angle α denotes the angle between the normal vector $\mathbf{z}$ at the contact point and the principal direction $\mathbf{e}$ of the tangent plane at that point. The dimensions and orientation of both the semi major axis and semi minor axis of the contact ellipses can be inferred from the curvature characteristics of the tooth surface:

$$a = \sqrt{\left|\frac{\delta}{K_\Sigma^1 - K_\Sigma^2 - \sqrt{g_1^2 - 2g_1 g_2 \cos 2\sigma + g_2^2}}\right|}, \tag{16}$$

$$b = \sqrt{\left|\frac{\delta}{K_\Sigma^1 - K_\Sigma^2 + \sqrt{g_1^2 - 2g_1 g_2 \cos 2\sigma + g_2^2}}\right|}, \tag{17}$$

$$\alpha = \frac{1}{2}\arccos\frac{g_1 - g_2 \cos 2\sigma}{\sqrt{g_1^2 - 2g_1 g_2 \cos 2\sigma + g_2^2}} \tag{18}$$

$$K_\Sigma^1 + K_\Sigma^2 = g_1 - g_2 \cos 2\sigma. \tag{19}$$

Given that tooth contact analyses are typically conducted under light load conditions, the elastic deformation δ in Eq. (16) to Eq. (17) is typically assumed to be 0.00025 inch, or 0.00632 mm. K_Σ^1 and K_Σ^2 are obtained by adding K_1 and K_2 for the pinion and the gear, g_1 and g_2 are obtained by subtracting K_2 from K_1 for the pinion and the gear, respectively. Figure 6 illustrates the variation in contact ellipses of the modified beveloid gear pair throughout the meshing process.

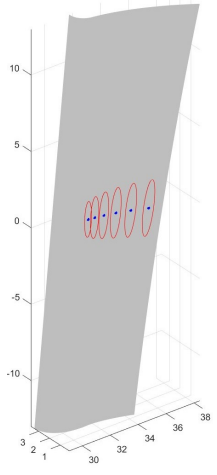

Fig. 6. Tooth contact ellipses

Figure 7 illustrates the variation in the area of the contact ellipses over time for different modification magnitudes. It can be observed that an increase in the magnitude of the modification results in a reduction in the contact ellipse area, which consequently gives rise

to an augmentation in the contact stress experienced by the tooth surface.

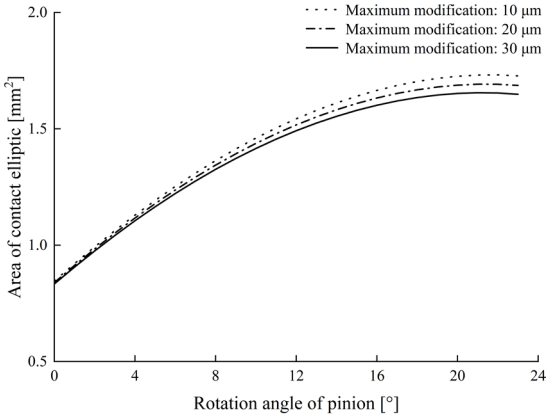

Fig. 7. Changes in the contact ellipse area

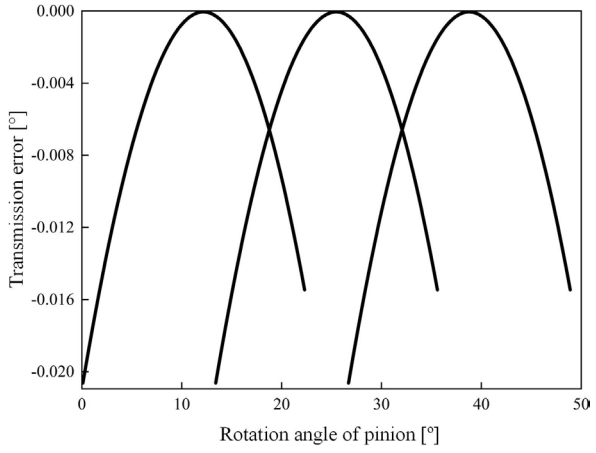

Fig. 8. Theoretical transmission error

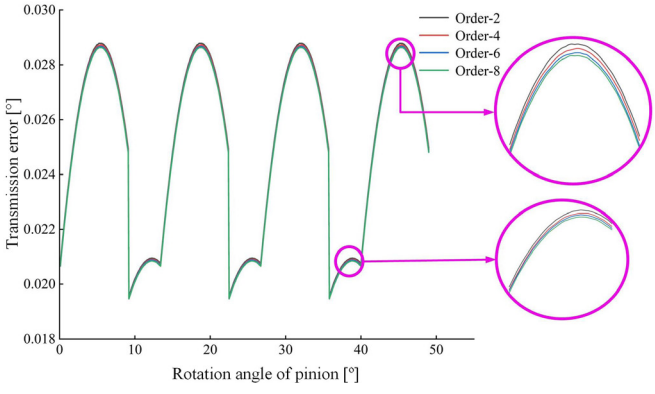

Fig. 9. Transmission error of beveloid gear pair

In conjunction with the tooth contact trajectory, the theoretical transmission error of the modified beveloid gear pair in the transmission process can be derived [21], as illustrated in Fig. 8. Figure 9 illustrates the cumulative transmission error of the beveloid gear pair following the superimposition of the transmission error of a single pair of teeth under varying modification curves. Figure 10 depicts the corresponding peak-to-peak transmission error. It can be observed that an increase in the order of the modification curve is associated with a reduction in the transmission error of the beveloid gear pair. This is accompanied by a decrease in the peak-to-peak value of the transmission error, which is conducive to the smooth transmission of the gear pair.

3.2 Influence of Assembly Error on Contact Characteristics of Involute Beveloid Gear with High-Order Curve Axial Modification

In involute beveloid gear pair, three principal forms of assembly errors may occur: center distance error, shaft staggering error, and shaft intersection angle error. These are illustrated in Fig. 11.

In the event of a solitary assembly error, the positive and negative assembly errors exert an opposing influence on the meshing path, while the impact of center distance errors is comparatively negligible. In the event of equality between the error values, the shaft intersection angle error exerts a more pronounced influence on the meshing path than the shaft staggering error.

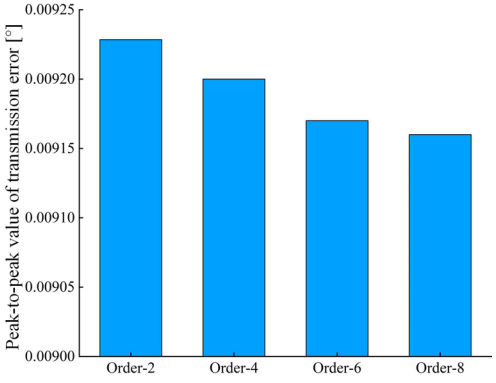

Fig. 10. Peak-to-peak value of the transmission error of beveloid gear pair

In order to investigate the impact of assembly errors on the meshing characteristics of the beveloid gear pair, a series of assembly errors have been introduced into the calculation of tooth contact analysis, with the resulting contact paths and contact ellipses illustrated in Fig. 12.

Figure 13 illustrates the variation in transmission error for the beveloid gear pair in the presence of a center distance error of 0.5 mm, a shaft staggering error of 0.3°, and a shaft intersection angle error of 0.3°, respectively. Figure 14 depicts the peak-to-peak value of transmission error for the aforementioned three cases. It can

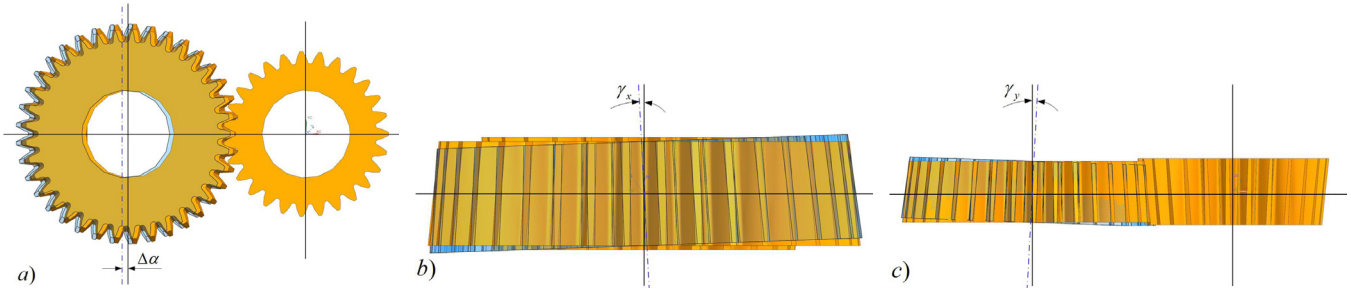

Fig. 11. The forms of assembly errors of beveloid gear pair; a) center distance error; b) shaft staggering error; and c) shaft intersection angle error

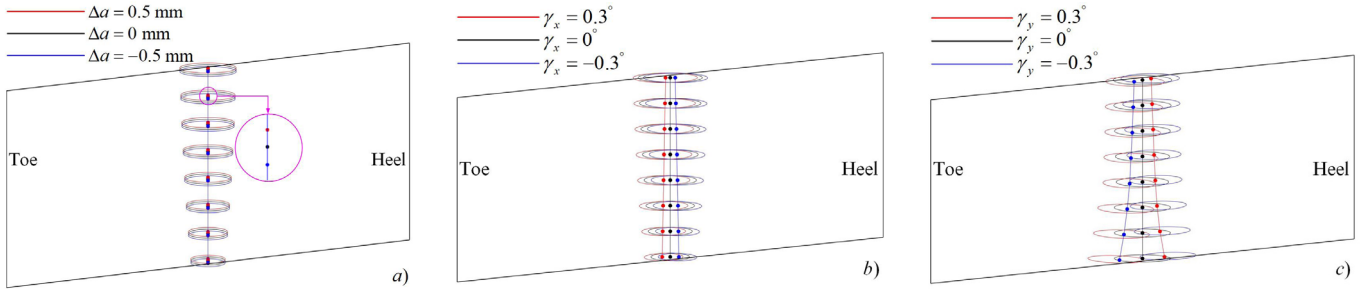

Fig. 12. Contact paths and contact ellipses of the beveloid gear pair with assembly errors; a) center distance error; b) shaft staggering error; and c) shaft intersection angle error

be observed that any assembly error results in an increase in the transmission error of the beveloid gear pair, with the peak-to-peak value also being affected. The largest increase in transmission error is caused by the presence of shaft intersection angle error, while the largest increase in the peak-to-peak value of transmission error is caused by the presence of shaft staggering error.

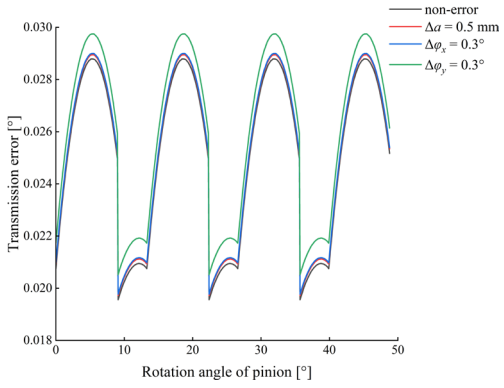

Fig. 13. Transmission error of beveloid gear pair with assembly errors

The combination of the results of the aforementioned analyses indicates that the beveloid gear pair with high-order curve axial modification exhibits superior tolerance performance with regard to center distance error and shaft staggering error. Conversely, the tolerance performance with respect to shaft intersection angle error is relatively poor.

Based on the aforementioned analysis, the transmission characteristics of the variable thickness gear pair were simulated using simulation software. The resulting transmission error, as depicted in Fig. 15, exhibits a trend that is largely consistent with the theoretical transmission error. This finding corroborates the accuracy and reliability of the analytical method presented in this study.

The beveloid gear pair with high-order curve axial modification shows strong tolerance to center distance error and shaft staggering error, but it is relatively poorly tolerated for shaft intersection error. The shaft intersection error can cause the contact point of gear meshing to shift, leading to significant transmission errors and uneven load distribution. This not only affects the stability and accuracy of the system but also reduces the service life of the gears. Consequently, while beveloid gears with high-order curve axial modified can tolerate other forms of assembly errors to some extent, their sensitivity to shaft intersection errors necessitates more precise control and compensation strategies in practical engineering applications.

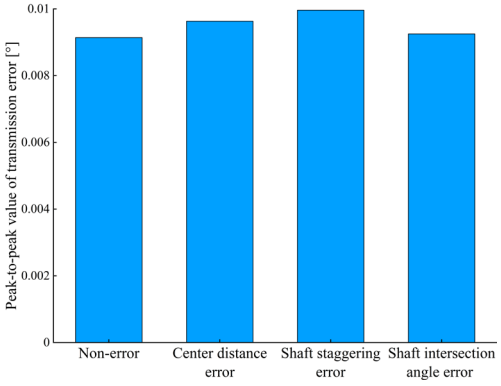

Fig. 14. Peak-to-peak value of transmission error of the beveloid gear pair with assembly errors

4 CONCLUSIONS

This paper presents a modelling and analysis of a beveloid gear pair with high-order curve axial modification. The conclusions drawn from this analysis are as follows:

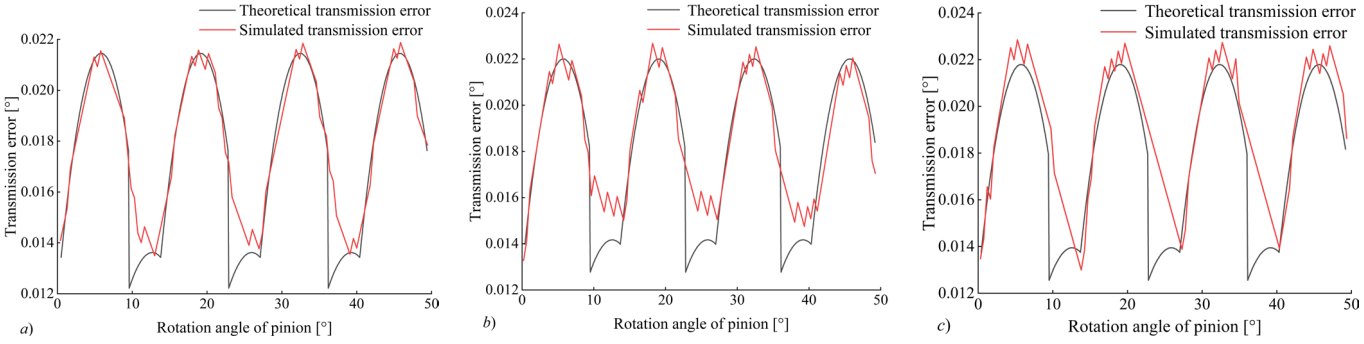

Fig. 15. Theoretical transmission error and simulated transmission error of beveloid gear pair with assembly errors; a) center distance error; b) shaft staggering error; and c) shaft intersection angle error

1. Following the axial modification, the tooth surface of the beveloid gear pair exhibits point contact. The contact trace is concentrated in the middle of the tooth surface, and the contact ellipse gradually increases from the root to the top of the tooth, before decreasing with the increase of the maximum amount of modification. This affects the smoothness of transmission of the gear pair.
2. It can be observed that an increase in the order of the modification curve is associated with a reduction in the transmission error of the beveloid gear pair. Consequently, the peak-to-peak value of the transmission error is also diminished.
3. The transmission error of the beveloid gear pair and its peak-to-peak values are observed to increase in the presence of assembly error. Conversely, the effect is observed to be smaller in the presence of center distance error and shaft staggering error. The largest effect is observed to occur in the presence of shaft intersection angle error.

References

[1] Wang, C., Cui, H., Zhang, Q., Zhang, B. Theoretical research progress of gear meshing efficiency. *J Univ Jinan (Sci. & Tech.)* 29 229-235 (2015) **DOI:10.13349/j.cnki.jdxbn.2015.03.014**.

[2] Chen, Q., Song, C., Zhu, C., Du, X., Ni, G. Manufacturing and contact characteristics analysis of internal straight beveloid gear pair. *Mech Mach Theory* 114 60-73 (2016) **DOI:10.1016/j.mechmachtheory.2017.04.002**.

[3] Sun, R., Song, C., Zhu, C., Wang, Y., Liu, K. Numerical study on contact force of paralleled beveloid gears using minimum potential energy theory. *J Strain Anal Eng Des* 56 249-264 (2020) **DOI:10.1177/0309324720936894**.

[4] Şentürk, B., Fetvaci, M. Modelling and undercutting analysis of beveloid gears. *J Fac Eng Archit Gaz* 35, 901-916 (2020) **DOI:10.17341/gazimmfd.544038**.

[5] Wen, J., Yao, H., Yan, Q., You, B. Research on time-varying meshing stiffness of marine beveloid gear system. *Mathematics* 11, 47-74 (2023) **DOI:10.3390/math11234774**.

[6] Song, C., Zhou, S., Zhu, C., Yang, X., Li, Z., Sun, R. Modeling and analysis of mesh stiffness for straight beveloid gear with parallel axes based on potential energy method. *J Adv Mech Des Syst Manuf* 12, 1-14 (2018) **DOI:10.1299/jamdsm.2018jamdsm0122**.

[7] Zhou, C., Dong, X., Wang, H., Liu, Z. Time-varying mesh stiffness model of a modified gear-rack drive with tooth friction and wear. *J Braz Soc Mech Sci* 44 213 (2022) **DOI:10.1007/S40430-022-03517-8**.

[8] Mao, H., Fu, L., Yu, G., Tupolev, V., Liu, W. Numerical calculation of meshing stiffness for beveloid gear with profile modification. *Compute Integra Manuf Sys* 28 526-535 (2022) DOI:10.13196/j.cims.2022.02.017.

[9] Liu, Y., Ren, Z., Wei, Y., Ma, D., Wei, S. Error study of involute beveloid spur gear transmission. *Mach Tool Hydraulic* 51, 1-6 (2023) **DOI:10.3969/j.issn.1001-3881.2023.04.001**.

[10] Wang, C., Wang, S., Wang, G. A calculation method of tooth profile modification for tooth contact analysis technology. *J Braz Soc Mech Sci* 40, 1-9 (2018) **DOI:10.1007/s40430-018-1268-4**.

[11] Fuentes, A., Gonzalez-Perez, I., Hayasaka, K. Computerized design of conical involute gears with improved bearing contact and reduced noise and vibration. *VDI Bericht* 2108, 635-646 (2010).

[12] Şentürk, B., Fetvaci, M. Modelling and undercutting analysis of beveloid gears. *J Fac Eng Archit Gaz*, 35, 901-916 (2020) **DOI:10.17341/gazimmfd.544038**.

[13] Morikawa, K., Kumagai, K., Nagahara, M. Infuence of tooth flank modfication on tooth surface damage of conical involute gears. *Trans JSME* 81 1-8 (2015) **DOI:10.1299/transjsme.15-00311**.

[14] Brecher, C., Löpenhaus, C., Brimmers, J. Function-oriented torlerancing of tooth flank modifications of beveloid gears. *Procedia CIRP* 43 124-129 (2016) **DOI:10.1016/j.procir.2016.02.155**.

[15] Brimmers, J., Brecher, C., Löpenhaus, C. Potenzial von freien Flanken modifikationen für Beveloidverzahnungen. F*orschung im Ingenieurwesen* 81 83-94 (2017) **DOI:10.1007/s10010-017-0232-2**.

[16] Ni, G., Zhu, C., Song, C., Du, X., Zhou, Y. Tooth contact analysis of crossed beveloid gear transmission with parabolic modification. *Mech Mach Theory* 113 40-52 (2017) **DOI:10.1016/j.mechmachtheory.2017.03.004**.

[17] Liu, S., Song, C., Zhu, C., Ni, G. Effects of tooth modifications on mesh characteristics of crossed beveloid gear pair with small shaft angle. *Mech Mach Theory* 119 142-160 (2018) **DOI:10.1016/j.mechmachtheory.2017.09.007**.

[18] Cao, Y., Ni, G., Fang, Z., Liu, Z. Effects of cutter modification on the meshing characteristics of intersected beveloid gear and involute cylindrical gear. *J Phys Conf Ser* 2691 012-022 (2024) **DOI:10.1088/1742-6596/2691/1/012022**.

[19] Zhang, Y., Zhou, H., Duan, C., Wang, Z., Luo, H. Gear differential flank modification design method for low noise. *Stroj Vestn-J Mech E* 70 569-581 (2024) **DOI:10.5545/sv-jme.2024.1072**.

[20] Wang, X., Lu, J., Yang, S. Sensitivity analysis and optimization design of hypoid gears' contact pattern to misalignments. *J Zhejiang Univ-Sc A* 20 411-430 (2019) **DOI:10.1631/jzus.A1900021**.

[21] Dong, C., Yang, X., Li, D., Zhao, G., Liu, Y. Service Performance optimization and experimental study of a new W-W type non-circular planetary gear train. *Stroj Vestn-J Mech E* 70 128-140 (2024) **DOI:10.5545/sv-jme.2023.673**.

Acknowledgements *This research was funded by the National Natural Science Foundation of China No. 52265008; the Youth Science Foundation of Gansu Province, No. 23JRRA751; the Education Department of Gansu Province: University Teachers Innovation Fund No. 2023A-021; the Wenzhou Municipal Basic Scientific Research Project of China No. 2022G0145.*

Received: 2024-12-23, revised: 2025-03-14, accepted: 2025-04-09 as *Original Scientific Paper.*

Data Availability *The data that support the findings of this study are available from the corresponding author upon reasonable request.*

Author Contribution *Yongping Liu: Data curation, Qi Chen: Writing–original draft preparation, Changbin Dong: Writing–review & editing.*

Analiza zobnega kontakta evolventnega stožčastega zobnika na osnovi aksialne modifikacije s krivuljo višjega reda

Povzetek *V tej raziskavi so preučene kontaktne značilnosti bokov zob evolventnega stožčastega zobniškega para z vidika aksialne modifikacije zobne površine s krivuljo višjega reda. Postavljen je koordinatni sistem obdelave modificiranega zobniškega para, izpeljane pa so tudi enačbe zobnih površin, ki temeljijo na principu zobniškega ubiranja in koordinatnih transformacijah. Izvedena je analiza kontakta modificiranega zobnika, pri čemer so preučeni vplivi spreminjajočih se parametrov na kontaktno sled in kontaktne elipse ter posledice za lastnosti ubiranja ob prisotnosti montažnih napak. Ugotovitve kažejo, da je oblika kontakta pri aksialni modifikaciji s krivuljo višjega reda pri stožčastem zobniškem paru v obliki točke. Poleg tega maksimalna velikost modifikacije in red krivulje modifikacije vplivata na lastnosti ubiranja stožčastega zobniškega para. Stožčasti zobniški par izkazuje izboljšano toleranco glede napake medosne razdalje in napake križanja osi, obenem pa kaže manjšo toleranco do napake presečišča osi.*

Ključne besede *evolventni stožčasti zobnik, aksialna modifikacija s krivuljo višjega reda, analiza zobnega kontakta, napaka prenosa, napaka pri montaži*